

## Stable Holographic Gratings with Small-Molecular Trisazobenzene Derivatives

Klaus Kreger,<sup>†</sup> Pascal Wolfer,<sup>‡</sup> Hubert Audorff,<sup>§,||</sup> Lothar Kador,<sup>§,||</sup>  
Natalie Stingelin-Stutzmann,<sup>‡,⊥</sup> Paul Smith,<sup>‡</sup> and Hans-Werner Schmidt<sup>\*,†,||</sup>

*Macromolecular Chemistry I, Institute of Physics, and Bayreuther Institut für Makromolekülforschung (BIMF), University of Bayreuth, D-95440 Bayreuth, Germany, Department of Materials, ETH Zürich, CH-8093 Zürich, Switzerland, and Department of Materials, Imperial College London, London SW7 2AZ, United Kingdom*

Received May 29, 2009; E-mail: hans-werner.schmidt@uni-bayreuth.de

**Abstract:** We present a series of small-molecular trisazobenzene chromophores, including, for instance, 1,3,5-tris[4-[4-(4-cyanophenyl)azo]phenoxy]butyl]amino}benzene that feature a remarkably stable light-induced orientation in initially amorphous thin-film architectures. It is demonstrated that for optimal performance it is critical to design chemical structures that allow formation of both an amorphous and a liquid-crystalline phase. In the present approach, the liquid-crystalline feature was introduced by inserting decoupling spacers between a trifunctionalized benzene core and the three azobenzene moieties, as well as adding polar end groups to the latter. To compensate for the deleterious reduction of the glass transition temperature associated with the spacers in the compounds, polar units were incorporated between the benzene core and the side groups. Intriguingly, the molecular glasses that feature a latent liquid-crystalline phase display a remarkable “postdevelopment”, i.e., an increase of the amplitude of refractive index modulation in holographic experiments after writing of optical gratings is arrested, exceeding 20% for the previously mentioned derivative. Thus, these nonpolymeric, azobenzene-containing compounds presented in this work appear to be attractive candidates for fabrication of stable holographic volume gratings.

### Introduction

Owing to the rich photochemistry of azobenzene chromophores, a large variety of both small-molecular and polymeric compounds have been synthesized for use as smart light-responsive materials in various potential applications.<sup>1</sup> One feature of azobenzene-containing species is their well-known *trans*-to-*cis* isomerization.<sup>2,3</sup> In addition, exposure to linearly polarized light of thin films of these compounds leads to in-plane orientation of chromophores by repeated *trans*-*cis*-*trans* isomerization cycles.<sup>4–6</sup> In holographic experiments, photoinduced alignment in such thin-film architectures obtained with two superimposed lasers was extensively explored for use in high-density data storage.<sup>7–10</sup> On the basis

of this technique, optical gratings have been successfully inscribed and highly useful optical characteristics and long-term stability of light-induced orientation have been demonstrated for selected *macromolecular* species—especially those that feature liquid-crystalline (LC) phases.<sup>11,12</sup> By contrast, related *small-molecular* compounds have been less explored. The latter have the advantage, among other things, of relatively simple synthesis, being of higher purity, resulting in well-defined structures and corresponding physicochemical properties and providing the option of homogeneously incorporating them into polymeric matrixes. Hence, in this study we set out to focus on those azobenzene chromophores of low molecular weight and in particular those that are prone to form molecular glasses.

Molecular glasses represent an emerging class of materials which are particularly investigated for potential application in optoelectronic devices, photoconductor drums, and photolithography.<sup>13–17</sup> These compounds combine high glass transition temperatures ( $T_g$ ) with pronounced—critically important—stable amorphous phases.<sup>18–20</sup> According to Naito et al., these features are met by small molecules exhibiting low entropic contributions, resulting in a high  $T_g$ , and low enthalpic contribu-

<sup>†</sup> Macromolecular Chemistry I, University of Bayreuth.

<sup>‡</sup> ETH Zürich.

<sup>§</sup> Institute of Physics, University of Bayreuth.

<sup>||</sup> BIMF, University of Bayreuth.

<sup>⊥</sup> Imperial College London.

- (1) Zhao, Y.; Ikeda, T. *Smart Light-Responsive Materials: Azobenzene-Containing Polymers and Liquid Crystals*; Wiley: Hoboken, NJ, 2009.
- (2) Rau, H. Photoisomerization of Azobenzenes. In *Photochemistry and Photophysics*; Rabek, J. F., Ed.; CRC Press: Boca Raton, FL, 1990; Vol. 2, p 119.
- (3) Zimmerman, G.; Chow, L.-Y.; Paik, U.-J. *J. Am. Chem. Soc.* **1958**, *80*, 3528.
- (4) Dumont, M. *Mol. Cryst. Liq. Cryst.* **1996**, *282*, 437.
- (5) Hagen, R.; Bieringer, T. *Adv. Mater.* **2001**, *13*, 1805.
- (6) Yager, K. G.; Barrett, C. J. *J. Photochem. Photobiol., A* **2006**, *182*, 250.
- (7) Eich, M.; Wendorff, J. H.; Reck, B.; Ringsdorf, H. *Macromol. Chem. Rapid Commun.* **1987**, *8*, 59.
- (8) Berg, R. H.; Hvilsted, S.; Ramanujam, P. S. *Nature* **1996**, *383*, 505.

- (9) Nikolova, L.; Todorov, T.; Ivanov, M.; Andruzzi, F.; Hvilsted, S.; Ramanujam, P. S. *Appl. Opt.* **1996**, *35*, 3835.
- (10) Sabi, Y.; Yamamoto, M.; Watanabe, H.; Bieringer, T.; Haarer, D.; Hagen, R.; Kostromine, S. G.; Berneth, H. *Jpn. J. Appl. Phys.* **2001**, *40*, 1613.
- (11) Natansohn, A.; Rochon, P. *Chem. Rev.* **2002**, *102*, 4139.
- (12) Hvilsted, S.; Andruzzi, F.; Kulinna, C.; Siesler, H. W.; Ramanujam, P. S. *Macromolecules* **1995**, *28*, 2172.

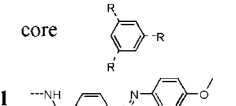
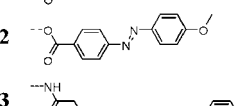
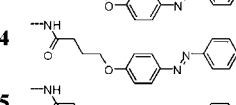
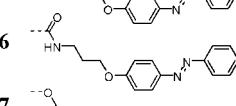
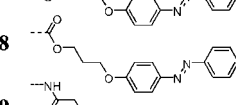
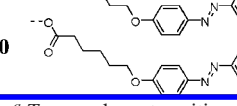
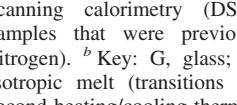
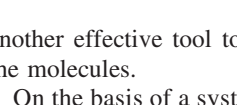
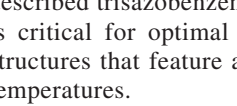
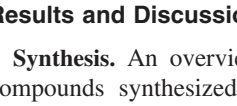
tions, minimizing the tendency for crystallization of a vitrified supercooled liquid.<sup>21,22</sup> Furthermore, it was demonstrated that hydrogen bonding between the molecular species may enhance the stability of an amorphous phase in thin films of small molecules.<sup>23</sup>

In recent years, *photochromic* molecular glasses have been investigated by several research groups with particular interest in the formation of surface relief gratings (SRGs).<sup>24–27</sup> In those studies, the light-induced mass transport over micrometer distances driven by the photoisomerization of the above-mentioned azobenzene moieties was demonstrated and characterized for the purposes of optical information storage and surface structuring. Recently, we investigated this feature for a series of azobenzene-containing molecular glasses, and structure–property relationships between the height of the SRGs and the optical susceptibility of the azobenzene moieties were unveiled.<sup>28</sup> Whereas those compounds were designed to efficiently form *surface relief gratings* with modulation heights up to 600 nm, practical use of azobenzene-containing molecular glasses for fabrication of *volume gratings* has been limited, since photoinduced molecular alignment in thin films typically was lost over a period of days or less. Owing to the promising optical performance, designing photochromic small molecules that can be applied for long-term stable volume gratings remains a challenge of fundamental interest.

On the basis of the design of molecular glasses featuring latent mesogenic character, we present azobenzene derivatives that are suitable for volume holographic data storage with remarkably stable gratings.

In the approach discussed, compounds that comprise three photoactive side groups that are linked, but decoupled with spacers of different lengths, to a central core in a  $C_3$ -symmetric pattern are synthesized.<sup>29</sup> Moreover, two trisazobenzene derivatives were prepared as reference compounds in which the chromophores are linked directly to the core. To compensate the reduction of the glass transition temperatures due to the decoupling spacers, polar moieties, i.e., amides or esters, were incorporated between the side groups and the core. Especially, the first—exhibiting the potential to form hydrogen bonds—will lead to higher glass transition temperatures as well as melting points. In addition to spacers, introduction of terminal dipolar substituents, e.g., methoxy or cyano groups, was employed as

**Table 1.** Chemical Structures and Thermal Properties of the Trisazobenzene Trisamides and Trisazobenzene Triesters Explored

compound	$T_g$ (°C) <sup>a</sup>	transition temperatures (°C) <sup>b</sup>
	134	G $\xrightleftharpoons[134]{187/233}$ Cr $\xrightleftharpoons[305]{}$ Iso
	65	Cr $\xrightleftharpoons[109]{163}$ Iso
	68	G $\xrightleftharpoons[68]{114/156}$ Cr $\xrightleftharpoons[192]{}$ Iso
	64	Cr $\xrightleftharpoons[155]{232}$ LC $\xrightleftharpoons[167]{}$ Iso
	68	Cr $\xrightleftharpoons[132]{251}$ LC $\xrightleftharpoons[193]{}$ Iso
	78	Cr $\xrightleftharpoons[143]{225}$ LC $\xrightleftharpoons[180]{}$ Iso
	58	Cr $\xrightleftharpoons[112]{162}$ LC $\xrightleftharpoons[146]{}$ Iso
	38	Cr $\xrightleftharpoons[126]{169}$ LC $\xrightleftharpoons[175]{177}$ Iso
	44	Cr $\xrightleftharpoons[114]{199}$ LC $\xrightleftharpoons[150]{}$ Iso
	40	Cr $\xrightleftharpoons[111]{150}$ LC $\xrightleftharpoons[138]{}$ Iso

<sup>a</sup>  $T_g$  = glass transition temperature (determined with differential scanning calorimetry (DSC) first-heating thermograms employing samples that were previously quenched from the melt in liquid nitrogen). <sup>b</sup> Key: G, glass; Cr, crystalline; LC, liquid-crystalline; Iso, isotropic melt (transitions correspond to peak temperatures of DSC second-heating/cooling thermograms).

another effective tool to enhance the mesogenic character of the molecules.

On the basis of a systematic study of a range of the above-described trisazobenzene derivatives, we demonstrate that it is critical for optimal holographic performance to design structures that feature a liquid-crystalline phase at elevated temperatures.

## Results and Discussion

**Synthesis.** An overview of the chemical structures of the compounds synthesized in this work is given in Table 1. Typically, three-arm star-shaped molecules were built up by either an amidation or an esterification reaction, both representing largely uncomplicated reaction types and, hence, conveniently allowing introduction of different polar groups or hydrogen-bonding moieties.

In detail, the molecules based on trisamide derivatives were synthesized by a 3-fold amidation of acid chlorides containing side groups together with 1,3,5-triaminobenzene. Molecules based on triester derivatives were obtained in a similar manner, however utilizing 1,3,5-trihydroxybenzene (cf. Scheme 1). When the molecules were based on 1,3,5-trimesic acid, i.e., when the direction of the amide or ester linkage was reversed, the photoactive side groups comprised amino groups or hydroxyl functions, respectively.

The design of the functional side groups was chosen in such a way that they could either be directly linked to the core or

- (13) Tang, C. W.; VanSlyke, S. A. *Appl. Phys. Lett.* **1987**, *51*, 913.
- (14) Bach, U.; Lupo, D.; Comte, P.; Moser, J. E.; Weissortel, F.; Salbeck, J.; Spreitzer, H.; Gratzel, M. *Nature* **1998**, *395*, 583.
- (15) Dai, J.; Chang, S. W.; Hamad, A.; Yang, D.; Felix, N.; Ober, C. K. *Chem. Mater.* **2006**, *18*, 3404.
- (16) De Silva, A.; Felix, N. M.; Ober, C. K. *Adv. Mater.* **2008**, *20*, 3355.
- (17) Van der Auweraer, M.; De Schryver, F. C.; Borsenberger, P. M.; Bassler, H. *Adv. Mater.* **1994**, *6*, 199.
- (18) Shirota, Y. *J. Mater. Chem.* **2000**, *10*, 1.
- (19) Strohrriegel, P.; Grazulevicius, J. V. *Adv. Mater.* **2002**, *14*, 1439.
- (20) Shirota, Y. *J. Mater. Chem.* **2005**, *15*, 75.
- (21) Naito, K.; Miura, A. *J. Phys. Chem.* **1993**, *97*, 6240.
- (22) Naito, K. *Chem. Mater.* **1994**, *6*, 2343.
- (23) Lebel, O.; Maris, T.; Perron, M.-E.; Demers, E.; Wuest, J. D. *J. Am. Chem. Soc.* **2006**, *128*, 10372.
- (24) Nakano, H.; Takahashi, T.; Kadota, T.; Shirota, Y. *Adv. Mater.* **2002**, *14*, 1157.
- (25) Chun, C.; Kim, M.-J.; Vak, D.; Kim, D. Y. *J. Mater. Chem.* **2003**, *13*, 2904.
- (26) Ishow, E.; Lebon, B.; He, Y.; Wang, X.; Bouteiller, L.; Galmiche, L.; Nakatani, K. *Chem. Mater.* **2006**, *18*, 1261.
- (27) Kim, M.-J.; Seo, E.-M.; Vak, D.; Kim, D.-Y. *Chem. Mater.* **2003**, *15*, 4021.
- (28) Audorff, H.; Walker, R.; Kador, L.; Schmidt, H.-W. *J. Phys. Chem. B* **2009**, *113*, 3379.
- (29) Junge, D. M.; McGrath, D. V. *J. Am. Chem. Soc.* **1999**, *121*, 4912.

Scheme 1. Overview of the Synthesis Routes to Trisazobenzene Trisamide and Trisazobenzene Triester Derivatives 1–10

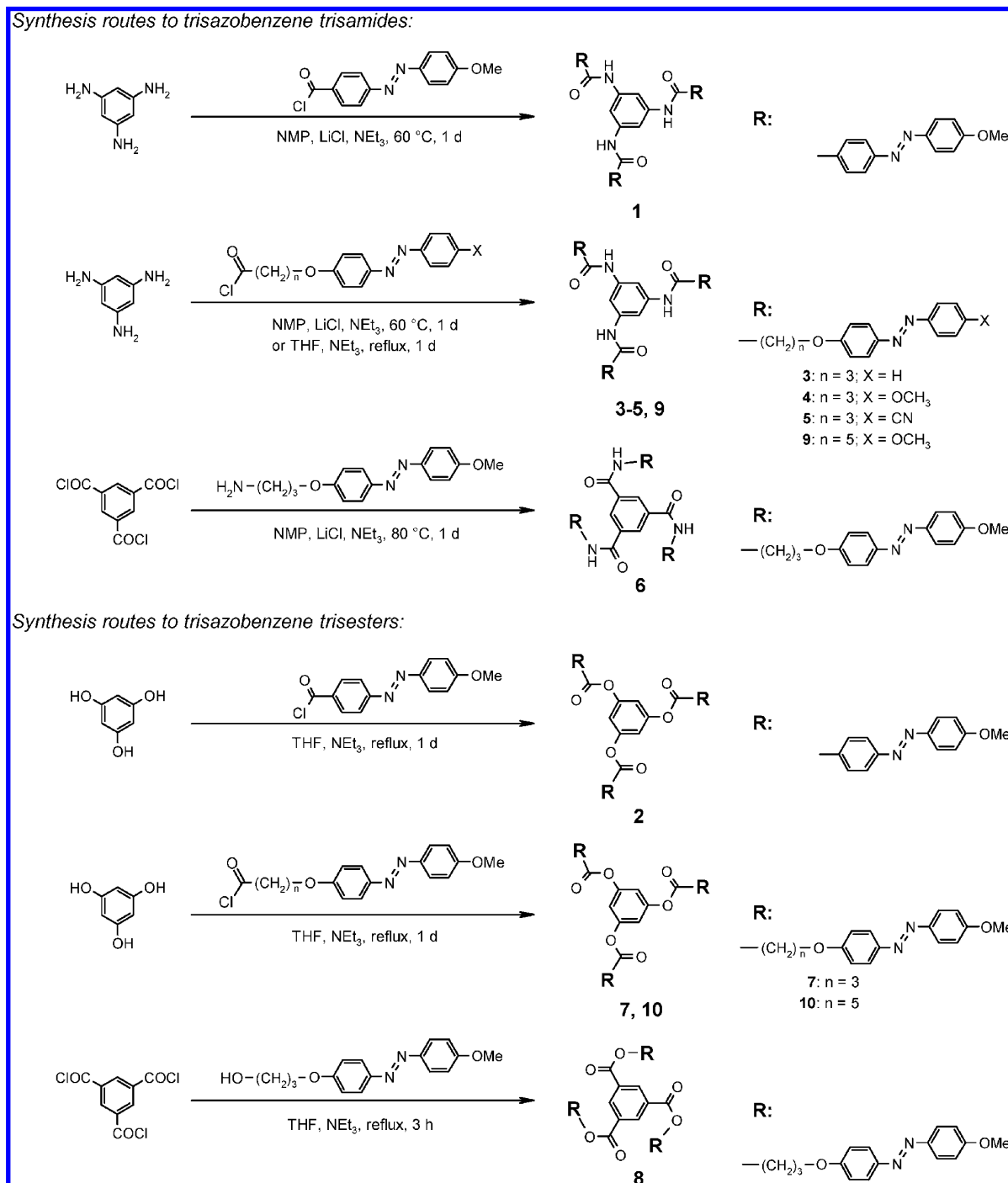
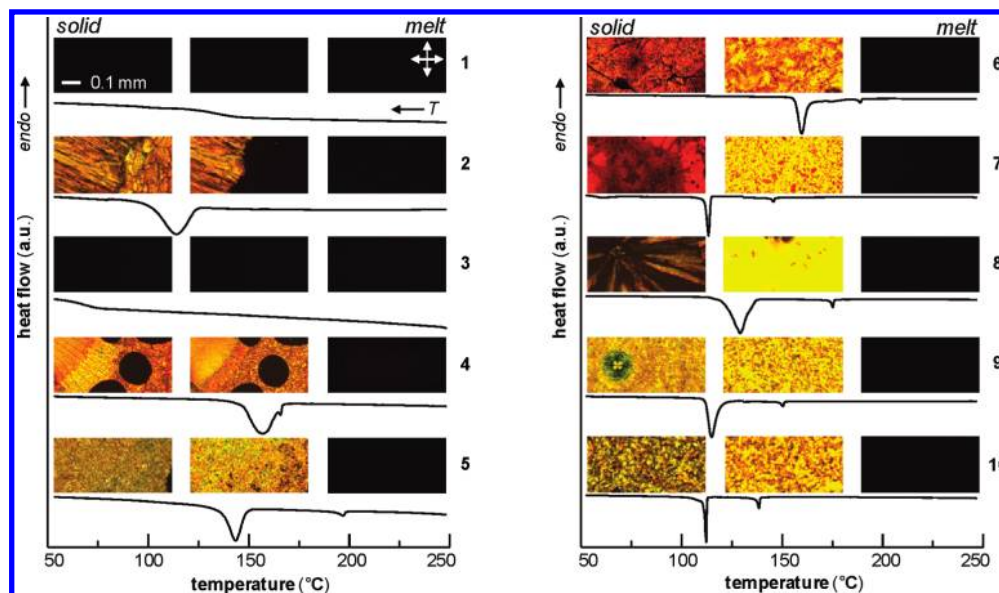


exhibit aliphatic spacers with three and five methylene units, effectuating a decoupling of the chromophores from the central core. In addition, different azobenzene chromophores were synthesized, i.e., azobenzene, (cyanoazo)benzene, and (methoxyazo)benzene derivatives. This set allowed the creation of several star-shaped compounds in a construction-kit principle where the required properties, e.g., the glass transition temperature, film-forming behavior, and photoactive characteristics, conveniently could be evaluated. In a typical procedure, the photoactive chromophores were formed by a common azo-coupling reaction. The aliphatic spacers with terminal ethyl esters were introduced by etherification and subsequent saponification to the corresponding acids. Azobenzene compounds with

carbonic acids were, finally, converted to reactive acid chloride species. In addition, side groups with amino or hydroxyl function in the spacer moieties were utilized if the core was based on trimesic acid derivatives. An amino function was obtained by introducing a *t*-Boc-protected aminopropyl spacer with subsequent cleavage of the protecting group, whereas in the case of hydroxyl-functionalized spacer moieties bromopropanol was used as the reagent for the etherification (for details see the Supporting Information). Mono- and bisubstituted products, as well as residual photochromic side groups, were analyzed by thin-layer chromatography (TLC) and oligomeric size-exclusion chromatography (SEC). Subsequently, they were removed by common techniques, e.g., flash chromatography and recrystal-



**Figure 1.** Differential scanning calorimetry (second-cooling thermograms, recorded under a  $N_2$  atmosphere at a rate of  $10\text{ }^\circ\text{C}/\text{min}$ ) and corresponding variable-temperature polarizing optical microscopy of the trisazobenzene derivatives indicate a liquid-crystalline phase for compounds **4–10** (polarizer/analyzer position illustrated with white arrows). Representative images were taken, respectively, above, between, and below the relevant transition temperatures.

lization. Especially, oligomeric SEC was found to be a powerful tool to monitor the reaction progress. From the monosubstituted to the trissubstituted species isolated peaks can be observed due to the increase of their hydrodynamic volume. All compounds were fully characterized by  $^1\text{H}$  nuclear magnetic resonance (NMR),  $^{13}\text{C}$  NMR, infrared (IR) spectroscopy, and elemental analysis (EA).

**Thermal Properties.** The thermal properties of the trisazobenzene derivatives were explored with differential scanning calorimetry (DSC) and supported by variable-temperature polarizing optical microscopy. The results of these studies are presented in Table 1 and Figure 1. In general, higher glass transition ( $T_g$ ), melting ( $T_m$ ), and crystallization ( $T_c$ ) temperatures were found for the amide homologues when compared to their ester counterparts. This difference illustrates the influence of a potential hydrogen bond formation in the former species. With increasing spacer length, however, this feature is reduced and, owing to strongly increased conformational arrangement possibilities, the influence of the spacers becomes more dominant, leading to a reduction in glass transition temperature with increasing length, as observed for compound series **1, 4, and 9** and **2, 7, and 10**. All trisazobenzene derivatives discussed featured a  $T_g$  above ambient, and hence, quenching to room temperature resulted in the formation of thermodynamic nonequilibrium amorphous glasses that were found to be stable at ambient conditions. All compounds that were designed with decoupling spacers between the central core and the side groups, i.e., **4–10**, had liquid-crystalline mesophases featured when they were cooled from the isotropic phase at a relatively moderate rate of  $10\text{ }^\circ\text{C}/\text{min}$  (cf. Table 1 and Figure 1). The values of the isotropic to liquid-crystalline transition enthalpies were found to be relatively small and ranged from  $-1.2$  to  $-4.0$  kJ/mol. In combination with typical defects in the Schlieren textures as observed in the polarizing microscope, this suggests the presence of nematic phases for trisazobenzenes **4–10**. When the compounds were heated from the solidified state at the same rate, on the other hand, only compound **8** featured an

LC phase prior to melting. In contrast to species **4–10**, compounds **1** and **3** displayed vitrification and the triester **2** was found to crystallize upon cooling. The above findings indicate that our design approach toward molecular glasses with liquid-crystalline character was successful with respect to thermal properties.

**Photochemical Behavior.** Determination of the photochemical behavior of the different compounds in tetrahydrofuran (THF) solutions, allowing us to study the *trans*-to-*cis* as well as the *cis*-to-*trans* isomerization, was employed as a first tool toward the optical characterization of thin films. Reassuringly, we found a strong photoresponse in solutions of all species in a series of ultraviolet/visible (UV/vis) light absorption spectra. This observation has its origin in the well-known *trans*-to-*cis* isomerization of the azobenzene moieties when exposed to unpolarized, monochromatic UV light. The photochemical reaction continued until a photostationary *cis*-rich state was reached. Subsequently, the corresponding back-relaxation to the thermodynamically more stable *trans* state was recorded when the samples were stored in the dark (Figure 2). Whereas during exposure to UV light the  $\pi,\pi^*$  absorbance decreased drastically, the  $n,\pi^*$  absorbance increased, while the reverse process occurred when the solutions were kept in the dark. Characteristically for reversible photochemical reactions, distinct isosbestic points were present in the sequences of UV/vis spectra.

**Holography.** For analyzing the suitability of the trisazobenzene derivatives for photoinduced volume gratings, their response in the solid state was investigated in a set of holographic experiments. To this end, thin, amorphous films were produced by spin-coating THF solutions of the azobenzene compounds. On the basis of this technique, films of good quality and homogeneous optical properties were fabricated. To increase the film thickness to a level required in holographic experiments, the viscosity of the solutions was enhanced by adding  $\sim 5$  wt % (with respect to the solute) ultra-high-molecular-weight polystyrene (UHMW-PS), resulting in active layers of  $\sim 400$  nm average thickness. In contrast to the UV light used for



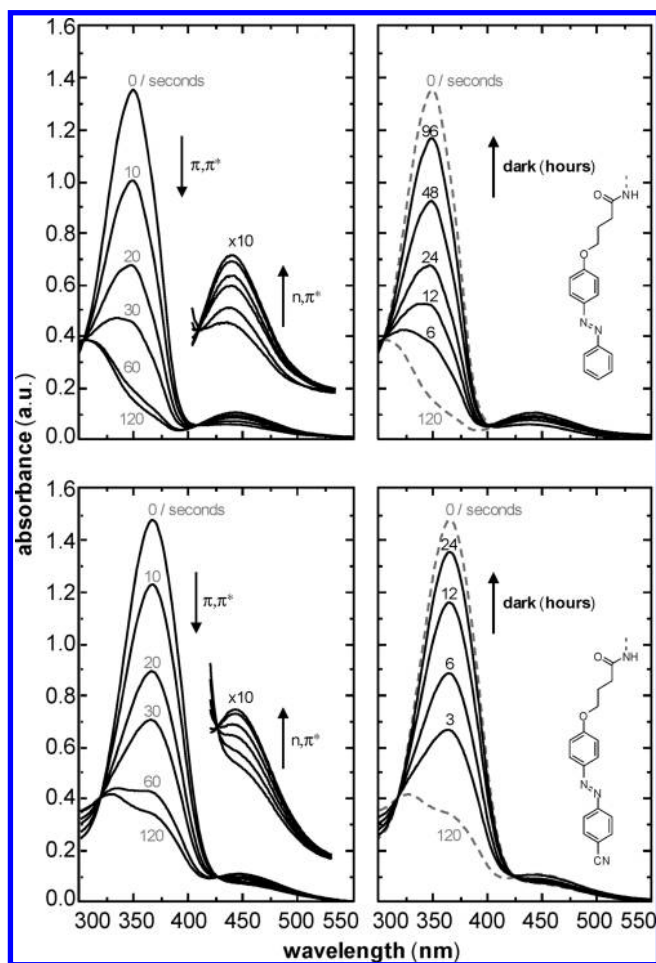


**Figure 2.** *cis*-to-*trans* isomerization of compounds **3** (top) and **5** (bottom) in THF solutions monitored with UV/vis spectroscopy: left, spectra taken after irradiation with UV light (365 nm) for different exposure times; right, thermal back-relaxation in the dark indicated in hours (solid lines), as well as spectra before and after 120 s of irradiation with UV light (dashed lines). The reversible character of the isomerization is emphasized by isosbestic points at 304 and 407 nm for derivative **3** and at 317 and 425 nm for compound **5**.

irradiating the solutions in the UV/vis examinations discussed above, here an argon ion laser at 488 nm was employed. Exposure to this source led to repeated *trans*-*cis*-*trans* isomerization cycles of the chromophores in the film. Hence, in-plane orientation of the azobenzene moieties perpendicular to the polarization of the interfering laser beams was induced in irradiated areas.

All compounds showed photo-orientation—here expressed as the amplitude of the refractive index modulation ( $n_1$ ) between oriented and nonoriented domains of the optical intensity gratings inscribed in holographic experiments. That optical characteristic was analyzed by the diffraction efficiency of the grating employing a laser diode of 685 nm wavelength, which is outside the absorption band of the azobenzene moieties, thus avoiding affecting the inscribed pattern. Details describing the experimental setup for the generation of holographic gratings have been published elsewhere.<sup>30</sup>

Typical for molecular glasses,  $n_1$  was found to decrease for **1**–**3** after the writing beams were shut off. However, most

**Table 2.** Refractive Index Modulation and Writing Time of Species **1**–**10**

	1	2	3	4	5	6	7	8	9	10
$n_1 \times 10^{-3}$ <sup>a</sup>	14	8	3	5	29	23	43	41	27	23
$t^b$ (s)	6	2	~0.5	8	5	20	~350	10	12	~200

<sup>a</sup> Maximum amplitude of refractive index modulation at inscription of holographic gratings. <sup>b</sup> Writing time to maximum of refractive index modulation (argon ion laser, 488 nm, 1 W/cm<sup>2</sup>).

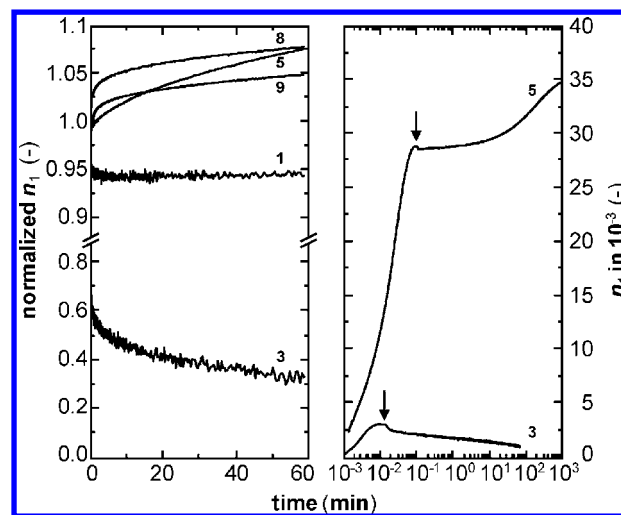


**Figure 3.** Refractive index modulation of ~400 nm thin films of small-molecular trisazobenzene compounds, prepared from THF solutions by spin-coating onto glass substrates, as a function of time: left, amplitude of refractive index modulation  $n_1$ , normalized to 1 when the writing laser was stopped, of **1**, **3**, **5**, **8**, and **9**; right, absolute values for **3** and **5** demonstrating the postdevelopment of the latter species on a logarithmic time scale (writing laser off indicated by arrows).

intriguingly, highly stable photo-orientation was observed for **4**–**10**. These compounds, which feature spacers and additional terminal groups, also displayed a remarkable “postdevelopment”—i.e., an increase of  $n_1$  after writing of the holographic gratings was arrested—exceeding, for instance, 20% for derivative **5**. As a consequence of overexposure and the resulting decrease of contrast between irradiated and unexposed areas, the refractive index modulation features a maximum during inscription. Thus, this amplification of  $n_1$  is a very useful tool for fabricating holographic intensity gratings with better contrast than achievable with optical writing methods only. To our knowledge, this highly beneficial phenomenon so far only has been reported for macromolecular systems.<sup>31,32</sup>

The present library of trisazobenzene compounds permitted us to conduct a cursory examination of the influence of certain key elements of the molecular architectures of these materials on their performance. Comparison of the characteristics of **1** and **2** with those of species **3**–**10**, for instance, demonstrates that the introduction of a spacer promotes, in most cases, the long-term stability of the photoinduced molecular alignment (cf. Table 2 and Figure 3).

An exception is compound **3**, which does not possess a polar end group and shows a rapid decay of the molecular orientation. This is in contrast to the behavior of all other spacer-decoupled

(30) Häckel, M.; Kador, L.; Kropp, D.; Schmidt, H.-W. *Adv. Mater.* **2007**, *19*, 227.

(31) Stumpe, J.; Läscher, L.; Fischer, T.; Rutloh, M.; Kostromin, S.; Ruhmann, R. *Thin Solid Films* **1996**, *284*–285, 252.

(32) Zilker, S. J.; Huber, M. R.; Bieringer, T.; Haarer, D. *Appl. Phys. B: Lasers Opt.* **1999**, *68*, 893.

azobenzene derivatives, indicating that these substituents have a positive effect on the stability of photoaligned patterns. Increasing spacer length, inversion of the amide or ester sequence in the side groups, and substitution of an amide by an ester or vice versa, did, however, not affect the presence of the stability but did have an effect on the absolute values of the refractive index modulation  $n_1$ , writing time  $t$  to a maximum of refractive index modulation, and degree of postdevelopment. Accordingly, the formation of hydrogen bonds in the amide homologues cannot be the origin of the observed stability found for selected species.

Whereas  $n_1$  typically was found to be higher for compounds featuring a liquid-crystalline phase at elevated temperatures, a clear correlation among  $n_1$ ,  $t$ , and the detailed molecular structure appears to be absent (cf. Table 2). Hence, the above observations suggest that two components, i.e., spacers and end groups, are crucial for stable photoinduced alignment of the trisazobenzene derivatives explored. Interestingly, we find that species featuring these specific architectural elements form molecular glasses with a latent liquid-crystalline phase (cf. Table 1 and Figure 3).

## Conclusions

In summary, azobenzene-containing low-molecular-weight compounds have been presented; those that feature liquid-crystalline behavior appear to be attractive nonpolymeric candidates for fabrication of stable holographic volume gratings. Different structural elements in the design of these star-shaped molecules allowed us to tailor the phase behavior of the compounds explored. Liquid-crystalline character was induced by integrating decoupling spacers between the benzene core and the three azobenzene moieties, as well as additional polar end groups. The glassy nature of the trisazobenzene derivatives was controlled with polar linkages, i.e., amide or ester bonds, between the core and the spacers. In solutions, reversible *trans*-to-*cis* isomerization was observed for all compounds. In a set of holographic experiments with amorphous films, however, stable intensity gratings only were obtained with species exhibiting decoupling spacers and additional end groups, i.e., liquid-crystalline molecular glasses **4–10**. For the same compounds an unusual postdevelopment of the refractive index modulation was demonstrated. By contrast, typical for molecular glasses, no stable volume gratings were obtained with reference compounds **1–3**, featuring either decoupling spacers or polar end groups only. These results indicate that it is critical for fabricating stable holographic gratings to design structures that feature liquid-crystalline behavior at elevated temperatures but still allow formation of stable amorphous films at ambient. Nevertheless, several characteristics observed in our investigations of the trisazobenzene derivatives, as well as the alignment mechanism on a molecular level, remain unclear and require further detailed studies.

## Experimental Section

**Materials.** The synthesis of 1,3,5-triaminobenzene is described elsewhere.<sup>33</sup> All other chemicals were commercially available from Aldrich and Acros and used without further purification. UHMW-PS ( $M_w \approx 30\,000$  kg/mol) was purchased from Polysciences, Inc., Warrington, PA. THF was refluxed for 3 days over CaH<sub>2</sub>, distilled, refluxed for another three days over potassium, and

finally distilled again. NMP was stirred for 3 days over CaH<sub>2</sub> and finally distilled off. Triethylamine was treated in the same manner. Phloroglucine, 1,3,5-benzenetricarbonyl trichloride, and (phenylazo)phenol, were commercially available.

**Characterization and Sample Preparation.** **Characterization Methods.** <sup>1</sup>H NMR and <sup>13</sup>C NMR spectra were recorded with a Bruker AC 300 spectrometer (300 and 75 MHz, respectively).

Fourier transform infrared (FTIR) spectra were recorded with a BIO-RAD Digilab FTS-40.

Oligomeric size exclusion chromatography (Oligo-SEC) measurements were performed utilizing a Waters 515-HPLC pump with stabilized THF as the eluent at a flow rate of 0.5 mL/min. A 20  $\mu$ L volume of a solution with a concentration of approximately 1 mg/mL was injected into a column setup, which consists of a guard column (Varian, 5  $\times$  0.8 cm, mesopore gel, particle size 3  $\mu$ m) and two separation columns (Varian, 30  $\times$  0.8 cm, mesopore gel, particle size 3  $\mu$ m). The compounds were monitored with a Waters 486 tunable UV detector at 254 nm and a Waters 410 differential RI detector.

EA was performed with a HEKAtech elemental analyzer, EA 3000 (Euro Vector CHNS), charged with tungsten oxide and copper. Detection was performed utilizing a GC setup equipped with a thermal conductivity detector.

DSC was conducted under a N<sub>2</sub> atmosphere at a scan rate of 10  $^{\circ}$ C/min with a Mettler Toledo DSC 822<sup>o</sup> instrument. For the determination of the glass transition temperatures  $T_g$  of the trisazobenzene derivatives explored, amounts of about 3 mg ( $\pm 0.2$  mg) each compound were sealed in Al standard 40  $\mu$ L crucibles, heated to 260  $^{\circ}$ C (except **1**, 310  $^{\circ}$ C), and subsequently quenched from the melt in liquid nitrogen. For all other phase transition temperatures, similar amounts were analyzed employing identical sample holders.

Glass transition temperatures  $T_g$  of all compounds were determined from DSC first heating thermograms of the melt-quenched samples. All other phase transitions were taken to be the peak temperatures in the DSC second-heating and -cooling thermograms.

**Thin-Film Preparation and Optical Analysis.** Thin films of all compounds were spin-coated at ambient with a Laurell WS-400B-6NPP/LITE spin-coater at 800 rpm from  $\sim 2$  wt % THF solutions (total content) onto glass slides. To increase the film thickness to a level required in holographic experiments,  $\sim 5$  wt % (with respect to the solute) UHMW-PS was added to the solutions.

UV/vis absorption spectra of about 0.01 mg/mL THF solutions of all compounds were recorded after different exposure times to UV light (365 nm) with a Perkin-Elmer Lambda 900 spectrophotometer. Subsequently, the thermal back-relaxation in the dark was analyzed in a second series of measurements.

Polarizing optical microscopy was carried out with a Leica DMRX polarizing microscope equipped with a Mettler Toledo FP82HT hot stage. The thermal behavior of the compounds was examined applying a continuous N<sub>2</sub> flow and a scan rate of 10  $^{\circ}$ C/min.

Holographic experiments were performed using the blue-green line (488 nm) of an argon ion laser. A beam splitter generated two coherent parts of the laser beam, which were brought to interference in the sample plane. The diameter of the s-polarized laser beams was about 1 mm; the intensity of each beam was adjusted to 0.5 W/cm<sup>2</sup>. The angle of incidence relative to the surface normal was  $\pm 14^{\circ}$ , resulting in a grating period of about 1  $\mu$ m. A laser diode at 685 nm, a wavelength range outside the absorption band of the azobenzene moiety, was used for in situ monitoring of the diffraction efficiency without affecting the writing process. To determine the diffraction efficiency of the grating, the powers of the transmitted and diffracted beams were measured with two photodiodes. For improving the signal-to-noise ratio, the laser diode was modulated and lock-in detection was used.

(33) Schmidt, H.-W.; Smith, P.; Blomenhofer, M. PCT Int. Appl. WO 02/46300A2, 2002.

**Synthesis and Characterization of Trisazobenzene Derivatives. General Preparation Method 1.** In a flame-dried flask 1.4 mmol of 1,3,5-triaminobenzene, 0.1 g of LiCl, and 1 mL of triethylamine were dissolved in 20 mL of dry NMP. Then the solution was cooled to 0 °C, and 4 equiv (5.5 mmol) of azobenzene-based acid chloride was added. The reaction mixture was allowed to warm to room temperature and subsequently stirred for 12 h at 60 °C. The solution was cooled to room temperature and poured into ice–water. The solid was filtered off and washed several times with water.

Trisamides based on trimesic acid were prepared in a similar manner.

**General Preparation Method 2.** In a flame-dried flask 1.4 mmol of phloroglucine and 1 mL of triethylamine were dissolved in 30 mL of dry THF. Then the solution was cooled to 0 °C, and 4 equiv (5.5 mmol) of 4-azobenzene-based acid chloride was added. The reaction mixture was allowed to warm to room temperature and refluxed for 12 h at 60 °C. The formed suspension was cooled to room temperature, and the triethylammonium salt was filtered off and washed several times with THF. Subsequently, the solvent was evaporated off.

Triesters based on trimesic acid were prepared in a similar manner.

**1,3,5-Benzenetrisamide Based on 1,3,5-Triaminobenzene.** The synthesis of 1,3,5-tris[[4-[(4-methoxyphenyl)azo]benzoyl]amino]benzene (**1**) was carried out according to general method 1. The crude product was recrystallized from THF/EtOH, yielding an orange solid (39%). <sup>1</sup>H NMR (DMSO-*d*<sub>6</sub>): δ = 3.88 (s, 9 H), 7.16 (d, 6 H), 7.96 (dd, 12 H), 8.13 (s, 3H), 8.20 (d, 6 H), 10.5 (s, 3H) ppm. <sup>13</sup>C NMR (DMSO-*d*<sub>6</sub>): δ = 56.6, 109.9, 115.6, 122.9, 125.8, 130.0, 137.2, 140.1, 147.1, 154.5, 163.2, 165.7 ppm. IR (KBr): 3308, 2838, 1654, 1600, 1540, 1503, 1418, 1258, 1139, 1052, 855, 836 cm<sup>-1</sup>. El. vol. (Oligo-GPC): 16.05 mL. Elemental analysis (N, C, H): calcd, 15.04, 68.81, 4.69; found, 14.44, 67.82, 4.76.

The synthesis of 1,3,5-tris[[4-[(phenylazo)phenoxy]butyryl]amino]benzene (**3**) was carried out according to general preparation method 1. After flash chromatography in ethyl acetate/cyclohexane (2/3) a yellow solid (yield 24%) was obtained. <sup>1</sup>H NMR (DMSO-*d*<sub>6</sub>): δ = 2.04 (quintet, 6 H), ~2.5 (6H), 4.10 (t, 6 H), 7.10 (d, 6 H), 7.5 (m, 9H), 7.66 (s, 3H), 7.83 (m, 12 H), 9.97 (s, 3H) ppm. <sup>13</sup>C NMR (DMSO-*d*<sub>6</sub>): δ = 24.6, 32.7, 67.4, 115.0, 122.2 (2C), 124.6, 129.3, 130.8, 139.5, 146.1, 152.0, 161.4, 170.6 ppm. IR (KBr): 3312, 3219, 3040, 2942, 2868, 1651, 1603, 1555, 1500, 1452, 1325, 1252, 1142, 1053, 839 cm<sup>-1</sup>. El. vol. (Oligo-GPC): 15.90 mL. Elemental analysis (N, C, H): calcd, 13.67, 70.34, 5.58; found, 13.19, 70.56, 5.69.

The synthesis of 1,3,5-tris[[4-[(4-methoxyphenyl)azo]phenoxy]butyryl]amino]benzene (**4**) was carried out according to general preparation method 1. After recrystallization from THF/MeOH a yellow solid (yield 32%) was obtained. <sup>1</sup>H NMR (DMSO-*d*<sub>6</sub>): δ = 2.05 (quintet, 6H), ~2.5 (6 H), 3.83 (s, 9H), 4.11 (t, 6 H), 7.09 (d, 12 H), 7.67 (s, 3H), 7.82 (m, 12 H), 9.97 (s, 3H) ppm. <sup>13</sup>C NMR (DMSO-*d*<sub>6</sub>): δ = 25.0, 33.0, 55.9, 67.8, 114.8, 115.3, 124.4 (2C), 139.8, 146.4, 146.5, 158.5, 161.1, 161.8, 171.0 ppm. IR (KBr): 3289, 3071, 1667, 1599, 1501, 1455, 1318, 1250, 1148, 1028, 941, 841 cm<sup>-1</sup>. El. vol. (Oligo-GPC): 15.73 mL. Elemental analysis (N, C, H): calcd, 12.45, 67.64, 5.68; found, 12.09, 67.13, 5.76.

The synthesis of 1,3,5-tris[[4-[(4-cyanophenyl)azo]phenoxy]butyryl]amino]benzene (**5**) was carried out according to general preparation method 1. After flash chromatography in THF/hexane (3/1) a yellow solid (yield 23%) was obtained. <sup>1</sup>H NMR (DMF-*d*<sub>7</sub>): δ = 2.19 (quintet, 6H), 2.65 (t, 6 H), 4.26 (t, 6 H), 7.23 (d, 6 H), 7.87 (s, 3H), 7.9–8.1 (m, 24 H), 10.06 (s, 3H) ppm. <sup>13</sup>C NMR (DMF-*d*<sub>7</sub>): δ = 25.2, 33.1, 68.3, 113.4, 115.6, 118.9, 123.4 (2C), 125.8, 134.2, 140.5, 147.0, 155.0, 163.2, 171.6 ppm. IR (KBr): 3341, 3090, 2844, 2226, 1698, 1599, 1501, 1418, 1254, 1138, 1043, 847 cm<sup>-1</sup>. El. vol. (Oligo-GPC): 15.48 mL. Elemental analysis (N, C, H): calcd, 16.86, 68.66, 4.85; found, 16.23, 68.53, 4.96.

The synthesis of 1,3,5-tris[[6-4-[(4-methoxyphenyl)azo]phenoxy]hexanoyl]amino]benzene (**9**) was carried out according to general preparation method 2, but performed at room temperature. Recrystallization from THF/EtOH yielded a yellow powder (87%). <sup>1</sup>H NMR (DMSO-*d*<sub>6</sub>): δ = 1.45 (m, 6H), 1.62 (m, 6 H), 1.74 (m, 6 H), 2.30 (t, 6 H), 3.82 (s, 9 H), 4.04 (t, 6 H), 7.06 (m, 12 H), 7.64 (s, 3H), 7.80 (m, 12 H), 9.86 (s, 3H) ppm. <sup>13</sup>C NMR (DMSO-*d*<sub>6</sub>): δ = 25.0, 25.1, 28.3, 36.3, 55.5, 67.8, 114.5, 114.9, 124.0, 124.1 (2C), 139.5, 146.0, 146.1, 160.9, 161.4, 171.2 ppm. IR (KBr): 3282, 3050, 2942, 1667, 1599, 1501, 1441, 1318, 1248, 1148, 1105, 1028, 841 cm<sup>-1</sup>. El. vol. (Oligo-GPC): 15.54 mL. Elemental analysis (N, C, H): calcd, 11.50, 69.02, 6.34; found, 11.00, 68.59, 6.49.

**1,3,5-Benzenetrisamide Based on 1,3,5-Trimesic Acid.** The synthesis of benzene-1,3,5-tricarboxylic acid tris[4-4-[(4-methoxyphenyl)azo]phenoxy]butyl]amide (**6**) was carried out according to general preparation method 1. After flash chromatography in THF/hexane (3/1) a yellow solid was obtained (yield 13%). <sup>1</sup>H NMR (DMSO-*d*<sub>6</sub>): δ = 2.03 (quintet, 6 H), 3.48 (m, 6 H), 3.83 (s, 9 H), 4.15 (t, 6 H), 7.09 (m, 12 H), 7.81 (m, 12H), 8.43 (s, 3 H), 8.84 (m, 3H) ppm. <sup>13</sup>C NMR (DMSO-*d*<sub>6</sub>): δ = 28.7, 36.5, 55.6, 66.7, 114.6, 115.0, 124.2 (2C), 128.6, 135.1, 146.1, 146.2, 160.9, 161.5, 165.7 ppm. IR (KBr): 3428, 3071, 2932, 2837, 1651, 1599, 1501, 1468, 1246, 1147, 1030, 841 cm<sup>-1</sup>. El. vol. (Oligo-GPC): 15.81 mL. Elemental analysis (N, C, H): calcd, 12.45, 67.64, 5.68; found, 11.48, 67.26, 5.99.

**1,3,5-Benzene Triester Based on 1,3,5-Trihydroxybenzene.** The synthesis of 1,3,5-tris[[4-[(4-methoxyphenyl)azo]benzoyl]oxy]benzene (**2**) was carried out according to general preparation method 2. The crude product was recrystallized from THF/EtOH, yielding an orange solid (50%). <sup>1</sup>H NMR (CDCl<sub>3</sub>): δ = 3.90 (s, 9 H), 7.03 (d, 6 H), 7.24 (s, 3H), 7.97 (dd, 12 H), 8.32 (d, 6 H) ppm. <sup>13</sup>C NMR (CDCl<sub>3</sub>): δ = 56.0, 114.7, 123.0, 125.7, 130.2, 131.7, 147.4, 151.9, 156.3, 163.2, 164.4, 166.5 ppm. IR (KBr): 3027, 2844, 1741, 1600, 1501, 1453, 1252, 1130, 1064, 835 cm<sup>-1</sup>. El. vol. (Oligo-GPC): 16.14 mL. Elemental analysis (N, C, H): calcd, 9.99, 68.57, 4.32; found, 9.83, 68.79, 4.40.

The synthesis of 1,3,5-tris[[4-[(4-methoxyphenyl)azo]phenoxy]butyryl]oxy]benzene (**7**) was carried out analogously to general preparation method 2, but performed at room temperature. After flash chromatography in CH<sub>2</sub>Cl<sub>2</sub>/THF (40/1) a yellow solid (yield 40%) was obtained. <sup>1</sup>H NMR (CDCl<sub>3</sub>): δ = 2.26 (quintet, 6H), 2.79 (t, 6 H), 3.89 (s, 9 H), 4.14 (t, 6 H), 6.86 (s, 3 H), 6.99 (m, 12H), 7.89 (m, 12 H) ppm. <sup>13</sup>C NMR (CDCl<sub>3</sub>): δ = 24.4, 30.9, 55.5, 66.7, 112.8, 114.1, 114.7, 124.3 (2C), 147.0, 147.1, 151.0, 160.7, 161.6, 170.8 ppm. IR (KBr): 3071, 2942, 2837, 1761, 1601, 1500, 1454, 1369, 1317, 1248, 1147, 1030, 943, 843 cm<sup>-1</sup>. El. vol. (Oligo-GPC): 15.78 mL. Elemental analysis (N, C, H): calcd, 8.28, 67.45, 5.36; found, 8.22, 67.37, 5.41.

The synthesis of 1,3,5-tris[[6-4-[(4-methoxyphenyl)azo]phenoxy]hexanoyl]oxy]benzene (**10**) was carried out according to general preparation method 2. Recrystallization from THF/EtOH yielded a yellow powder (86%). <sup>1</sup>H NMR (CDCl<sub>3</sub>): δ = 1.62 (m, 6 H), 1.84 (m, 12 H), 2.58 (t, 6 H), 3.87 (s, 9 H), 4.04 (t, 6 H), 6.84 (s, 3H), 6.98 (dd, 12 H), 7.87 (dd, 12 H) ppm. <sup>13</sup>C NMR (CDCl<sub>3</sub>): δ = 24.9, 26.0, 29.2, 34.6, 55.9, 68.2, 113.1, 114.5, 115.0, 124.7, 124.7, 147.3, 147.4, 151.5, 161.4, 161.9, 171.6 ppm. IR (KBr): 3050, 2942, 2870, 1765, 1599, 1501, 1462, 1422, 1318, 1250, 1127, 1024, 918, 843 cm<sup>-1</sup>. El. vol. (Oligo-GPC): 15.55 mL. Elemental analysis (N, C, H): calcd, 7.65, 68.84, 6.05; found: 7.61, 69.33, 6.23.

**1,3,5-Benzene Triester Based on 1,3,5-Trimesic Acid.** The synthesis of benzene-1,3,5-tricarboxylic acid tris[4-4-[(4-methoxyphenyl)azo]phenoxy]butyl] triester (**8**) was carried out according to general method 2. After flash chromatography in toluene/THF a yellow solid was obtained (yield 63%). <sup>1</sup>H NMR (CDCl<sub>3</sub>): δ = 2.32 (quintet, 6 H), 3.88 (s, 9 H), 4.20 (t, 6 H), 4.62 (t, 6 H), 7.00 (m, 12 H), 7.88 (m, 12 H), 8.87 (s, 3H) ppm. <sup>13</sup>C NMR (CDCl<sub>3</sub>): δ = 28.6, 29.7, 55.1, 62.9, 64.6, 114.1, 114.6, 124.3 (2C), 131.3, 134.6, 147.0, 147.1, 160.6, 161.6, 164.8 ppm. IR (KBr): 3073, 2965, 2880, 1730, 1599, 1500, 1421, 1319, 1236, 1147, 1028, 985, 839

cm<sup>-1</sup>. El. vol. (Oligo-GPC): 15.91 mL. Elemental analysis (N, C, H): calcd, 8.28, 67.45, 5.36; found, 8.01, 67.08, 5.47.

**Acknowledgment.** P.W. acknowledges the Materials Research Center (MRC) at ETH Zürich for initiating the project with seed funding. N.S.-S. thanks the Royal Society for a Seed Fund Research Grant. Financial support for this work at the University of Bayreuth by the German Science Foundation (Grant SFB 481, B2) is gratefully acknowledged. We are also indebted to S. Ganzleben,

D. Hanft, and C. Löffler for their invaluable assistance in material synthesis.

**Supporting Information Available:** Synthesis of side groups and additional figures. This material is available free of charge via the Internet at <http://pubs.acs.org>.

JA9091038